Deformable Model with Adaptive Mesh and Automated Topology Changes

Jacques-Olivier Lachaud

Benjamin Taton

Laboratoire Bordelais de Recherche en Informatique (LaBRI)

Outline

Motivations

Segmentation/Reconstruction of large 3D images.

- steady technical improvements of acquisition devices,
- increase of image resolution and hence of image size.

Motivations

Segmentation/Reconstruction of large 3D images.

Deformable templates, superquadrics,
Fourier snakes. . .

- reduced set of shape prameters ➠ robust and efficient,
- lack of genericity: new problem ➠ new model.

Motivations

Segmentation/Reconstruction of large 3D images.

Deformable templates, superquadrics, Fourier snakes. . . not generic enough

Fully generic models (T-Snakes, Simplex meshes, Level-sets. . .)

- very wide range of shapes,
- number of shape parameters directly determined by image resolution ➠ heavy computational costs.

Motivations

Segmentation/Reconstruction of large 3D images.	
Deformable templates, superquadrics, Fourier snakes. . .	not generic enough
Fully generic models (T-Snakes, Simplex meshes, Level-sets. . .)	computationally expensive

Objective

- To build a deformable model
  - that can recover objects with any topology,
  - with costs more independent from the size of input data.

Model Description

Explicit model

- Closed triangulated surface,
- Dynamics of a mass-spring system that undergoes
  - image forces,
  - regularizing internal forces,
  - any other additional force…

Model Description

Explicit model

- Closed triangulated surface,
- Dynamics of a mass-spring system that undergoes
  - image forces,
  - regularizing internal forces,
  - any other additional force…

Regular sampling
of the model mesh

Model Description

Explicit model

- Closed triangulated surface,
- Dynamics of a mass-spring system that undergoes
  - image forces,
  - regularizing internal forces,
  - any other additional force…

Regular sampling of the model mesh $\nearrow$ Transformed into adaptive sampling by changing metrics

Model Description

Explicit model

- Closed triangulated surface,
- Dynamics of a mass-spring system that undergoes
  - image forces,
  - regularizing internal forces,
  - any other additional force…

Regular sampling of the model mesh → Transformed into adaptive sampling by changing metrics

Regular sampling of the model mesh → Automated topology changes

Regular Sampling

Regular sampling using distance constraints

$$\delta \leq d_E(u, v) \leq \zeta\delta$$

Where

- u, v are neighbour vertices,
- d_E denotes the Euclidean distance,
- δ determines the global resolution of the model,
- ζ is the ratio between the lengths of the longest and smallest edge on the mesh.

Regular Sampling

Regular sampling using distance constraints

$$\delta \leq d_E(u,v) \leq \zeta\delta$$

Restoring constraints

Edge too short: contraction
(+ special case. . .)

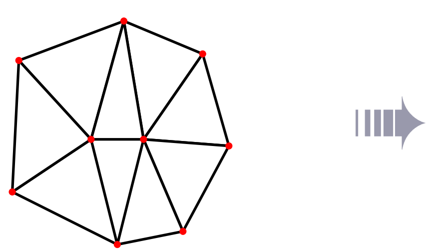

Edge too long: split

Resolution Adaptation

Euclidean distance replaced by a Riemannian distance

$$\delta \leq d_R(u, v) \leq \zeta\delta$$

Resolution Adaptation

Euclidean distance replaced by a Riemannian distance

$$\delta \leq d_R(u, v) \leq \zeta\delta$$

If d_R underestimates distances

edge lengths fall under the δ threshold

➠ edges contract and vertex density decreases.

Resolution Adaptation

Euclidean distance replaced by a Riemannian distance

$$\delta \leq d_R(u, v) \leq \zeta\delta$$

If d_R underestimates distances

edge lengths fall under the δ threshold
➠ edges contract and vertex density decreases.

If d_R overestimates distances

edge lengths exceed the $\zeta\delta$ threshold
➠ edges split and vertex density increases.

Resolution Adaptation

Euclidean distance replaced by a Riemannian distance

$$\delta \leq d_R(u, v) \leq \zeta\delta$$

The new distance d_R should

- overestimate distances in interesting parts of the image to increase accuracy,
- underestimate distances elsewhere to decrease accuracy.

Riemannian Metrics

Euclidean length of an elementary displacement $\vec{ds}$

$$L_E(\vec{ds}) = \sqrt{\vec{ds} \times {}^t\vec{ds}}$$

Riemannian Metrics

Riemannian length of an elementary displacement $\vec{ds}$

$$L_R(\vec{ds}) = \sqrt{\vec{ds} \times G(x_1, \ldots x_n) \times {}^t\vec{ds}}$$

Where G is a Riemannian metric, i.e.

- $G(x_1, \ldots x_n)$ is a dot product,
- G is continous.

Which means that $L_R(\vec{ds})$ depends on both

- the displacement $\vec{ds}$,
- the origin $(x_1, \ldots x_n)$ of the displacement.

Riemannian Metrics

Riemannian length of an elementary displacement $\vec{ds}$

$$L_R(\vec{ds}) = \sqrt{\vec{ds} \times G(x_1, \ldots x_n) \times {}^t\vec{ds}}$$

Length of a path γ

$$L_R(\gamma) = \int_0^1 \sqrt{\vec{\dot{\gamma}}(t) \times G(\gamma(t)) \times {}^t\vec{\dot{\gamma}}(t)}\, dt$$

Length of a path $\simeq$ Sum of the lengths of the elementary displacements it is composed of.

Riemannian Metrics

Riemannian length of an elementary displacement $\vec{ds}$

$$L_R(\vec{ds}) = \sqrt{\vec{ds} \times G(x_1, \ldots x_n) \times {}^t\vec{ds}}$$

Length of a path γ

$$L_R(\gamma) = \int_0^1 \sqrt{\vec{\dot{\gamma}}(t) \times G(\gamma(t)) \times {}^t\vec{\dot{\gamma}}(t)}\, dt$$

Distance between two points u and v

$$d_R(u, v) = \inf \left\{ L_R(\gamma) \,|\gamma(0) = u, \gamma(1) = v \right\}$$

Geometrical Interpretation of Metrics

Euclidean unit ball

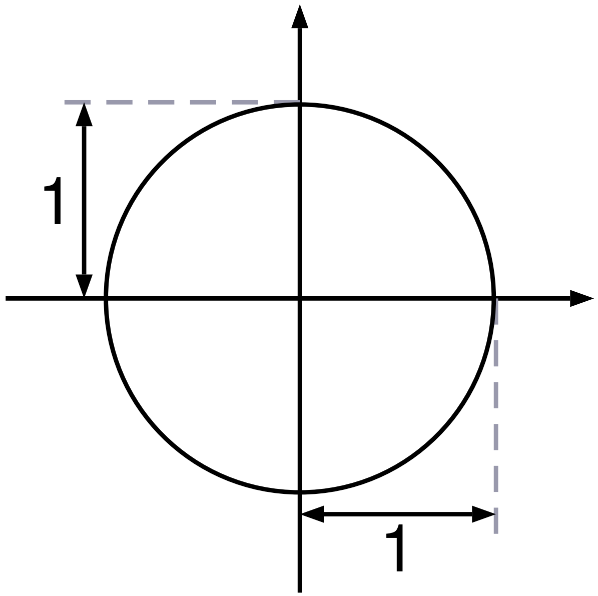

Local Riemannian unit ball

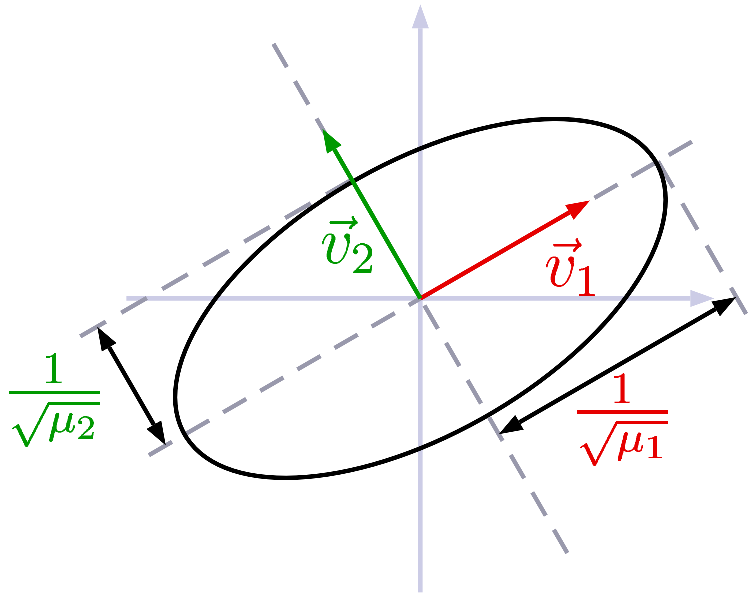

$(\vec{v}_1, \mu_1)$, $(\vec{v}_2, \mu_2)$ local eigen decomposition of the metric.

Geometrical Interpretation of Metrics

Euclidean unit ball

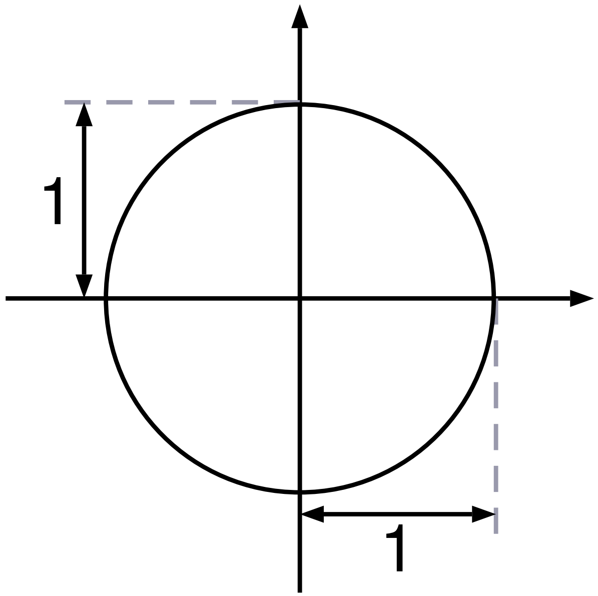

Local Riemannian unit ball

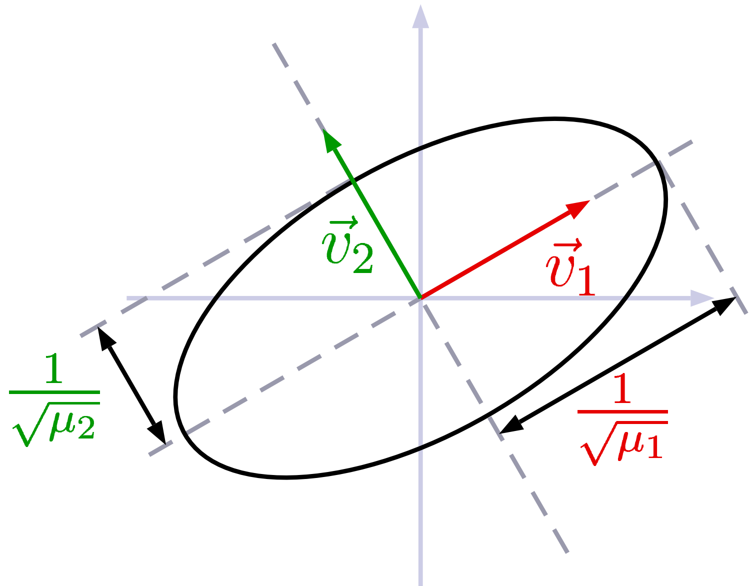

Changing the Euclidean metric with a Riemannian metric G

Locally expanding/contracting the space

Geometrical Interpretation of Metrics

Euclidean unit ball

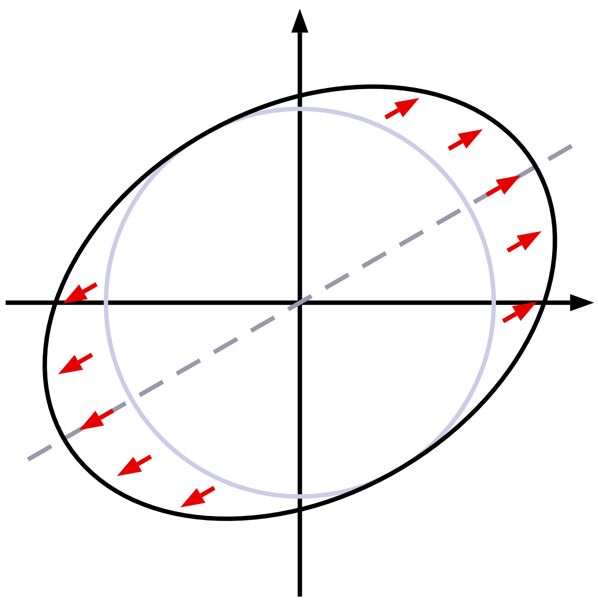

Local Riemannian unit ball

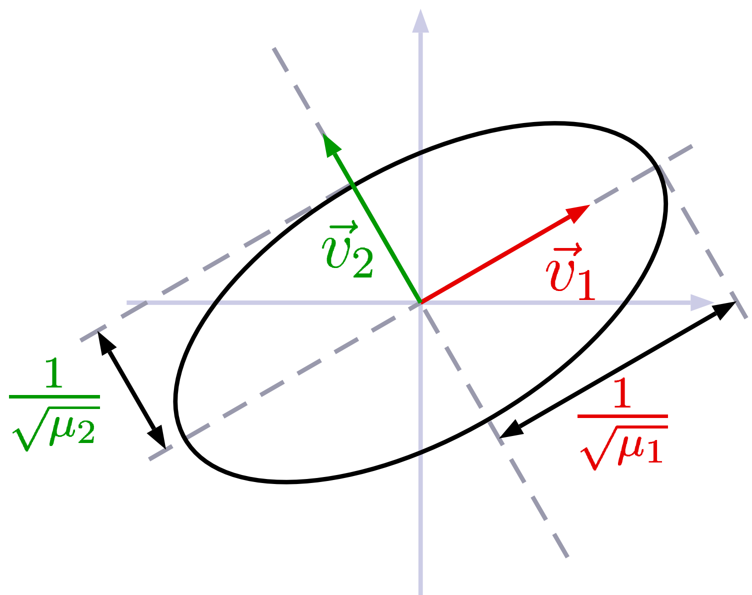

Changing the Euclidean metric with a Riemannian metric G

Locally expanding/contracting the space

along $\vec{v}_1$ with the ratio $\frac{1}{\sqrt{\mu_1}}$,

Geometrical Interpretation of Metrics

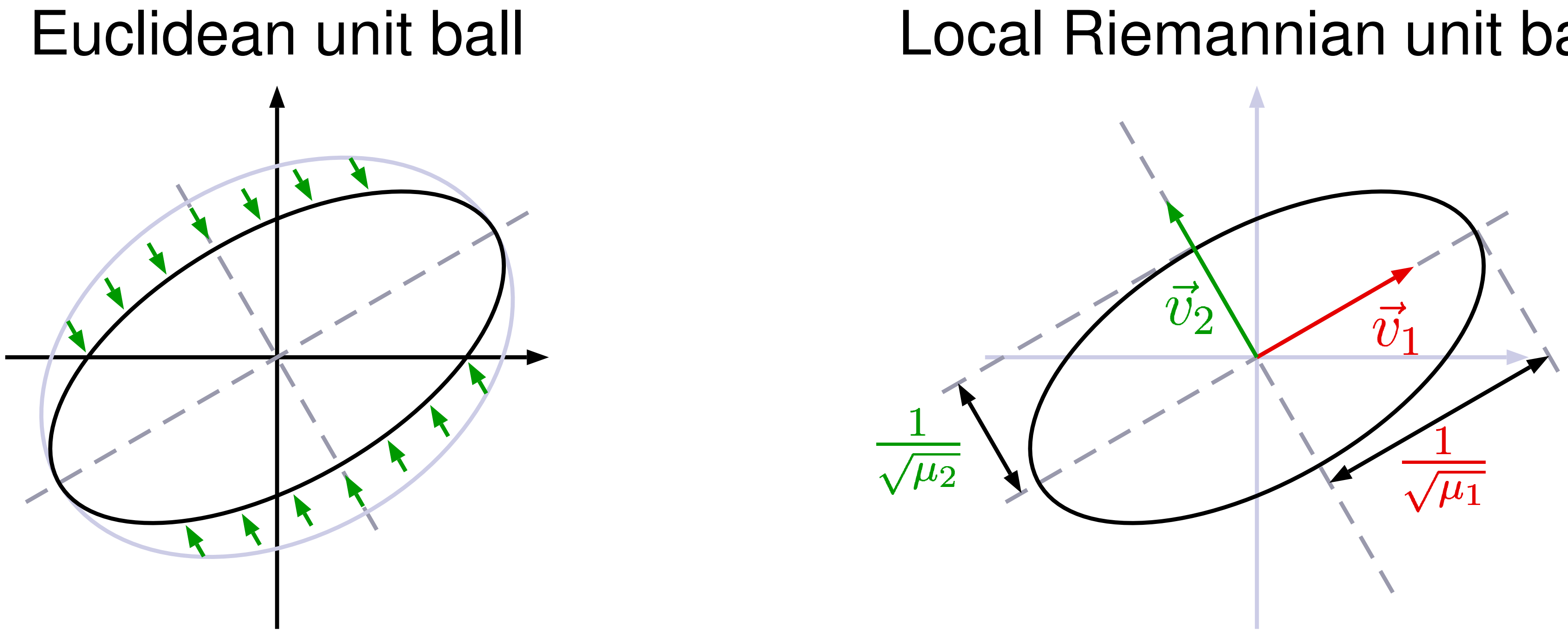

Changing the Euclidean metric with a Riemannian metric G

Locally expanding/contracting the space

along $\vec{v}_1$ with the ratio $\dfrac{1}{\sqrt{\mu_1}}$, along $\vec{v}_2$ with the ratio $\dfrac{1}{\sqrt{\mu_2}}$, ...

Topology Changes

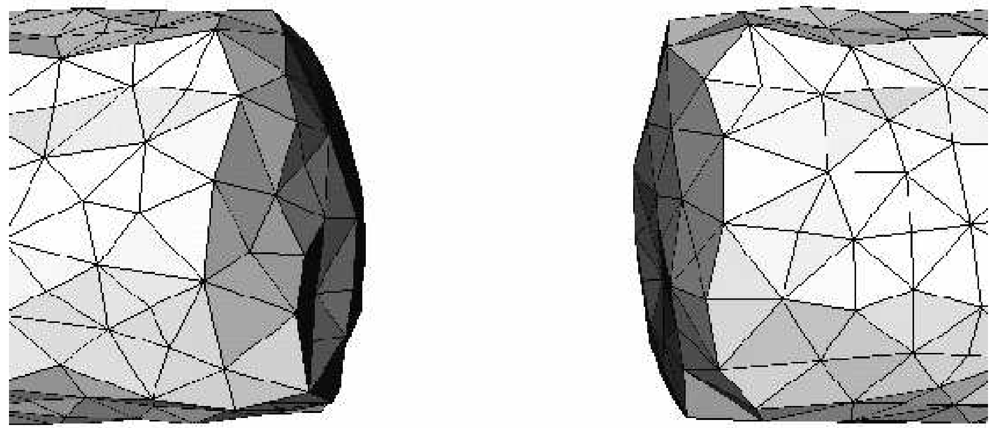

Two stages :

- ◇ detect self collisions of the model,
- ◇ perform appropriate local reconfigurations of the mesh.

Topology Changes

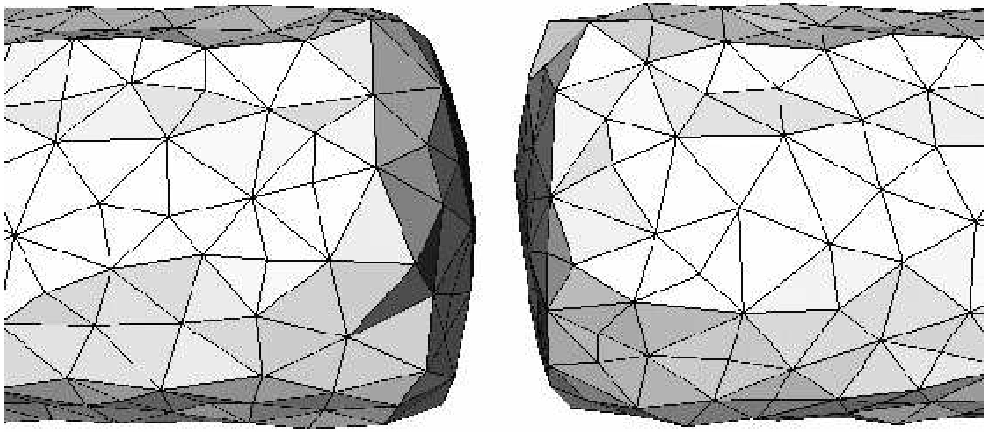

Two stages :

- ◇ detect self collisions of the model,
- ◇ perform appropriate local reconfigurations of the mesh.

Topology Changes

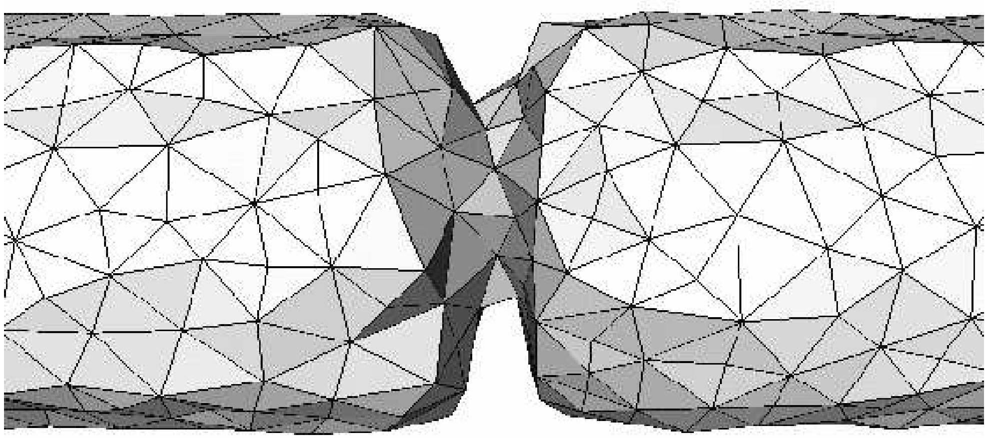

Two stages :

- detect self collisions of the model,
- perform appropriate local reconfigurations of the mesh.

Topology Changes

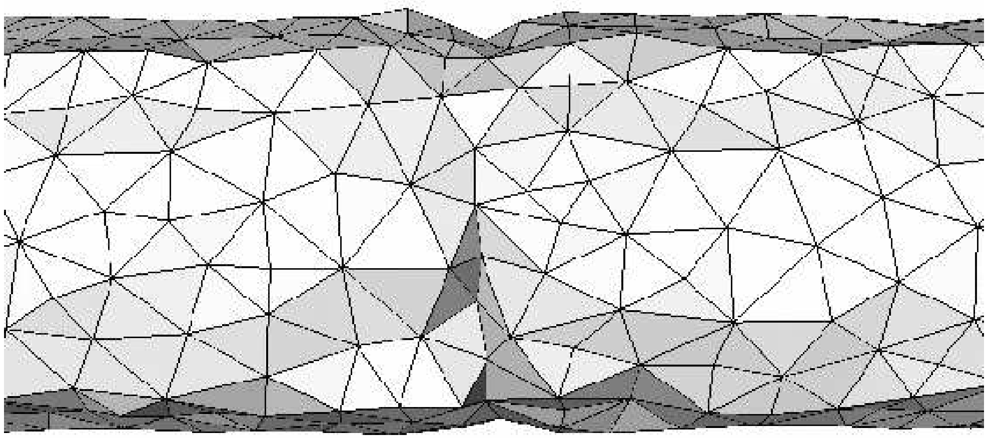

Two stages :

- detect self collisions of the model,
- perform appropriate local reconfigurations of the mesh.

Detection of self collisions

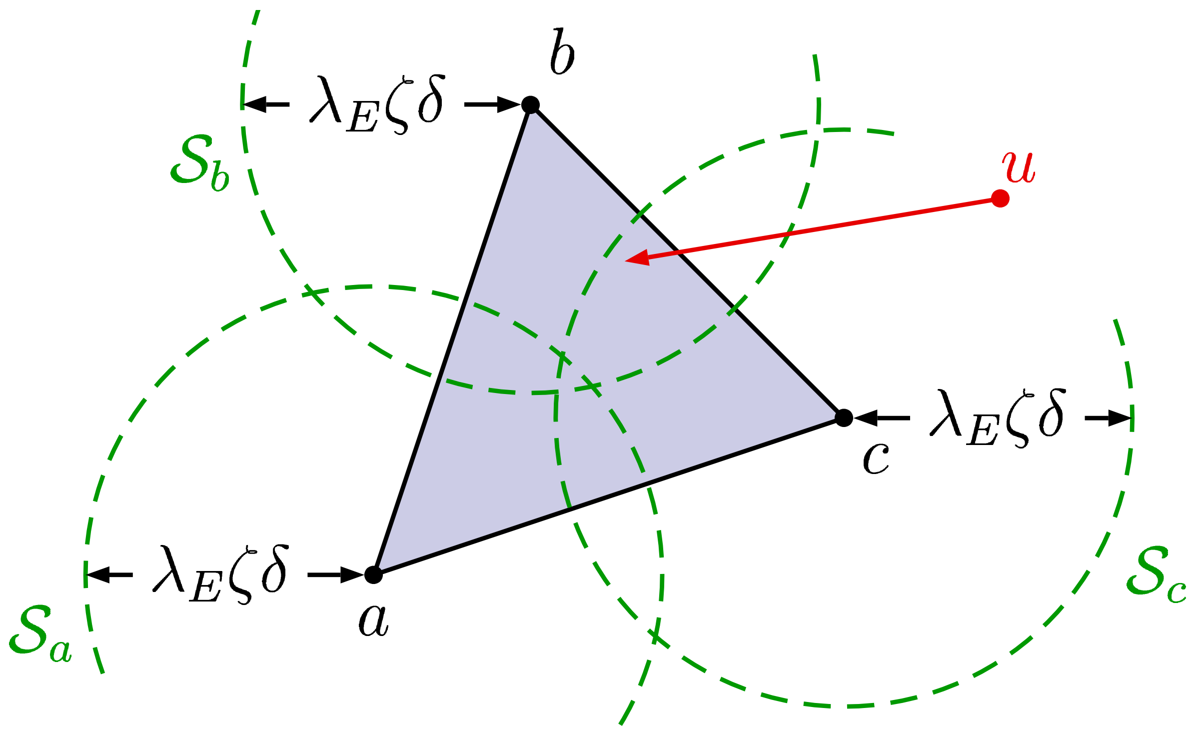

Vertex u crosses over the (a, b, c) face ⇒ Vertex u enters one of the $\mathcal{S}_a$, $\mathcal{S}_b$ or $\mathcal{S}_c$ spheres.

Topology Changes

Detection of self collisions

- Collision if u and w are not neighbours and $d_E(u, w) \leq \lambda_E \zeta \delta$.

Topology Changes

Detection of self collisions

◇ Collision if u and w are not neighbours and $d_E(u,w) \leq \lambda_E \zeta \delta$.

Local reconfigurations

Collision between two parts of the mesh

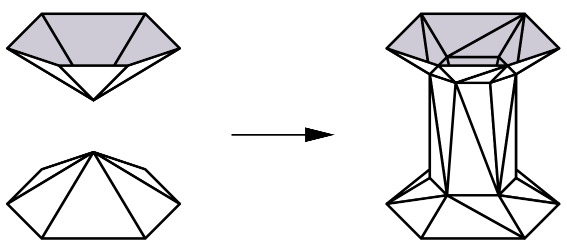

Special case of edge contraction

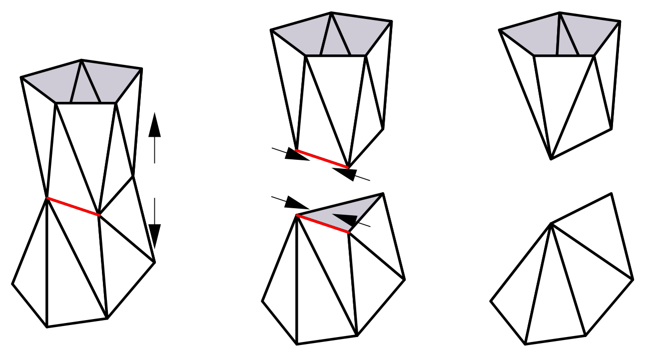

Topology Changes

Detection of self collisions

- ◇ Collision if u and w are not neighbours and $d_E(u,w) \leq \lambda_E \zeta \delta$.

Local reconfigurations

Collision between two parts of the mesh

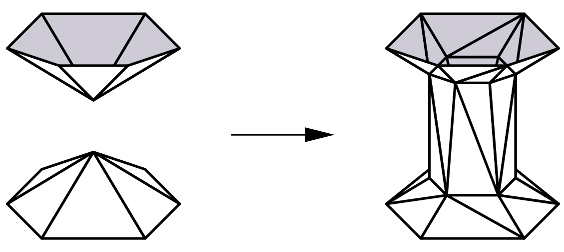

Special case of edge contraction

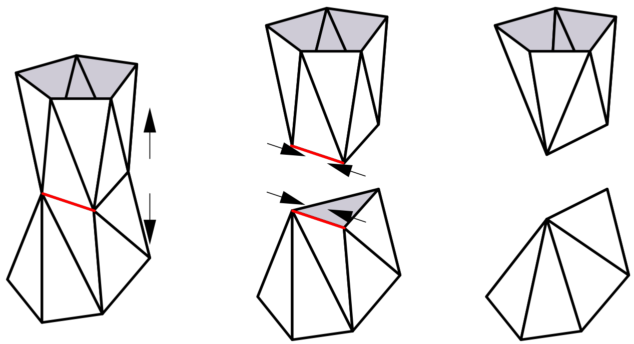

If the metric is changed

- ◇ λ_E replaced with a new constant λ_R

Dynamics

Motion equations with a Euclidean Metric

$$\forall k \in \{1, \ldots n\}, \quad m\ddot{x}_k = F_k$$

Dynamics

Motion equations with a Riemannian metric

$$\forall k \in \{1, \dots n\}, \quad m\ddot{x}_k = F_k - \sum_{i,j=1}^{n} \Gamma_{ij}^{k} \dot{x}_i \dot{x}_j$$

Addition of a corrective term that takes account of the metric

- $\Gamma_{ij}^{k} = \frac{1}{2} \sum_{l=1}^{n} g^{kl} \left(\frac{\partial g_{il}}{\partial x_j} + \frac{\partial g_{lj}}{\partial x_i} - \frac{\partial g_{ij}}{\partial x_l} \right)$ (Christoffel's symbols),
- g_{ij} are the coefficients of the $G(x_1, \dots x_n)$,
- g^{kl} are the coefficients of $G^{-1}(x_1, \dots x_n)$,

Dynamics

Motion equations with a Riemannian metric

$$\forall k \in \{1, \dots n\}, \quad m\ddot{x}_k = F_k - \sum_{i,j=1}^{n} \Gamma_{ij}^{k} \dot{x}_i \dot{x}_j$$

Addition of a corrective term that takes account of the metric

- $\Gamma_{ij}^{k} = \frac{1}{2} \sum_{l=1}^{n} g^{kl} \left(\frac{\partial g_{il}}{\partial x_j} + \frac{\partial g_{lj}}{\partial x_i} - \frac{\partial g_{ij}}{\partial x_l} \right)$ (Christoffel's symbols),
- g_{ij} are the coefficients of the $G(x_1, \dots x_n)$,
- g^{kl} are the coefficients of $G^{-1}(x_1, \dots x_n)$,

(corrective term neglected: second order in $\dot{x}$ + no influence on the rest position)

Summary

	Euclidean Metric	Riemannian Metric
Distance estimation	$\sqrt{\overrightarrow{uv} \times {}^t\overrightarrow{uv}}$	$\inf_{\gamma} L_R(\gamma)$
Regular sampling	$\delta \leq d_E(u,v) \leq \zeta\delta$ uniform resolution	$\delta \leq d_R(u,v) \leq \zeta\delta$ adaptive resolution
Collision detection	$d_E(u,v) \leq \lambda_E\zeta\delta$	$d_R(u,v) \leq \lambda_R\zeta\delta$
Local recon-figurations		unchanged
Motion equations	$m\ddot{x} = F$	$m\ddot{x}_k = F_k - \sum_{i,j=1}^{n} \Gamma_{ij}^k \dot{x}_i \dot{x}_j$

Required Properties

Four kinds of situations

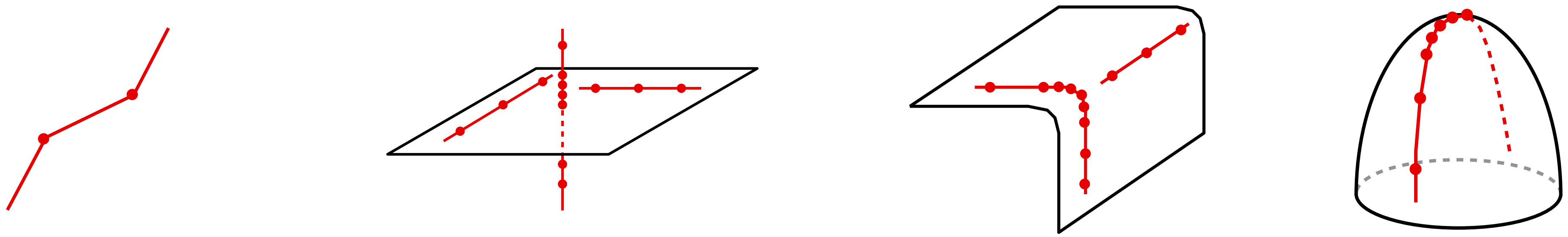

no contour — plane contour — edge, tubular structure — corner

Choice of the metric

- Eigenvectors should correspond the normal and the principal directions of the contour,
- Eigenvalues should correspond to the strength and the principal curvatures of the contour.

Required Properties

Structure in the image	Expected resolution	Eigen structure of the metric
No contour	◇ low in all directions	$0 \simeq \mu_2 \simeq \mu_1 \simeq \mu_0$
Flat contour	◇ low in the direction of the contour ◇ high in the orthogonal direction	$0 \simeq \mu_2 \simeq \mu_1 \ll \mu_0$
Tubular structure	◇ low in the direction of the structure ◇ high in both orthogonal directions	$0 \simeq \mu_2 \ll \mu_1 \simeq \mu_0$
Corner	◇ high along all directions	$0 \ll \mu_2 \simeq \mu_1 \simeq \mu_0$

Structure Tensor (1/2)

Definition

The matrix $J_{\rho,\sigma}$ that represents the mapping:

$$\vec{v} \quad \longrightarrow \quad g_\rho * \left(\vec{\nabla}(\, g_\sigma * I \,) \cdot \vec{v} \right)^2$$

Which results in:

$$J_{\rho,\sigma} = g_\rho * \begin{pmatrix} {I_x}^2 & I_x I_y & I_x I_z \\ I_x I_y & {I_y}^2 & I_y I_z \\ I_x I_z & I_y I_z & {I_z}^2 \end{pmatrix}$$

Structure Tensor (1/2)

Definition

The matrix $J_{\rho,\sigma}$ that represents the mapping:

$$\vec{v} \quad \longrightarrow \qquad\qquad g_\sigma * I \;) \cdot \vec{v} \;\Big)^2$$

Interpretation

- smoothes the input image,

Structure Tensor (1/2)

Definition

The matrix $J_{\rho,\sigma}$ that represents the mapping:

$$\vec{v} \quad \longrightarrow \qquad \vec{\nabla}(\; g_\sigma * I \;) \cdot \vec{v} \;\Big)^2$$

Interpretation

- ◇ smoothes the input image,
- ◇ characterizes direction and orientation of image gradient,

Structure Tensor (1/2)

Definition

The matrix $J_{\rho,\sigma}$ that represents the mapping:

$$\vec{v} \quad \longrightarrow \qquad \left(\vec{\nabla}(\, g_\sigma * I \,) \cdot \vec{v} \right)^2$$

Interpretation

- smoothes the input image,
- characterizes direction and orientation of image gradient,
- removes the orientation information,

Structure Tensor (1/2)

Definition

The matrix $J_{\rho,\sigma}$ that represents the mapping:

$$\vec{v} \quad \longrightarrow \quad g_\rho * \left(\vec{\nabla}(\, g_\sigma * I \,) \cdot \vec{v} \right)^2$$

Interpretation

- smoothes the input image,
- characterizes direction and orientation of image gradient,
- removes the orientation information,
- integrates the direction information over a neighbourhood.

Structure Tensor (2/2)

Properties of the eigenstructure of the structure tensor

In the neighbourhood of a contour

- $\vec{v}_1$ orthogonal to image contours, ξ_1 contour strength,
- $\vec{v}_2$, $\vec{v}_3$ principal directions of the contour, ξ_2 and ξ_3 qualitatively equivalent to principal curvatures.

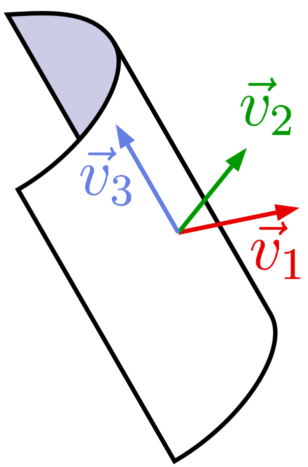

no contour	0	$\simeq$	ξ_3	$\simeq$	ξ_2	$\simeq$	ξ_1
flat contour	0	$\simeq$	ξ_3	$\simeq$	ξ_2	$\ll$	ξ_1
sharp edge	0	$\simeq$	ξ_3	$\ll$	ξ_2	$\simeq$	ξ_1
corner	0	$\ll$	ξ_3	$\simeq$	ξ_2	$\simeq$	ξ_1

Results (1/3)

Computer generated image

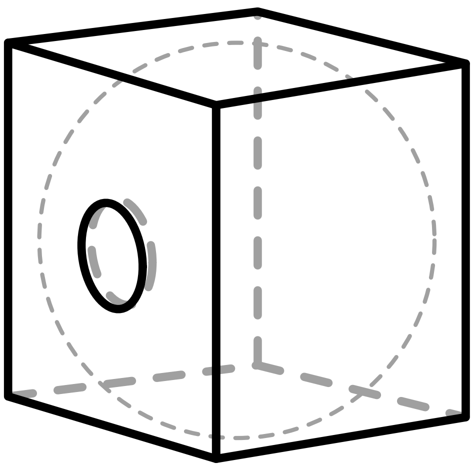

Object represented in the image

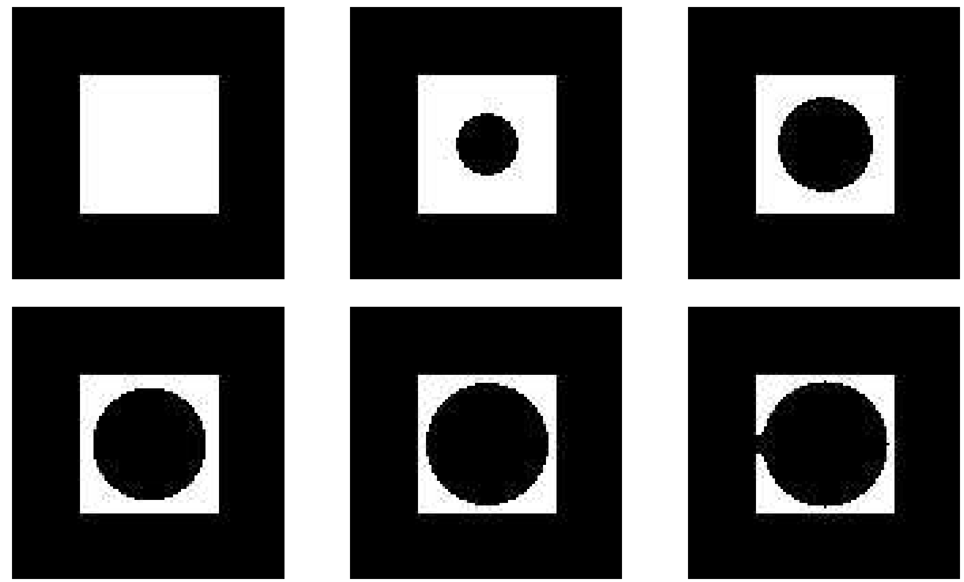

Slices extracted from the image

Results (1/3)

Eigen decomposition of the structure tensor

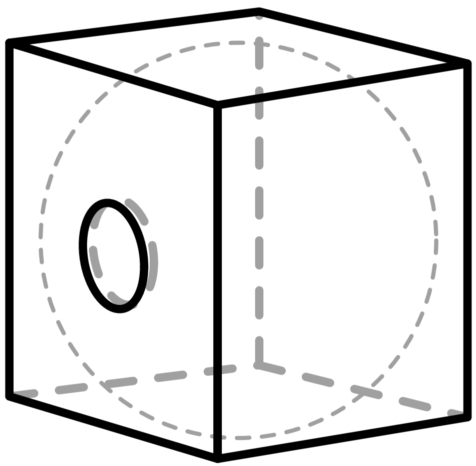

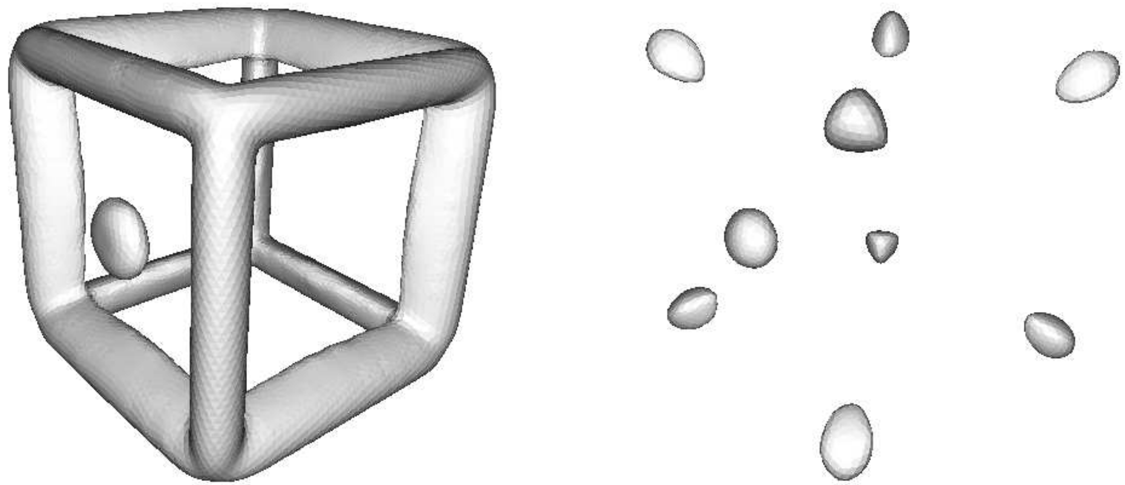

Object represented in the image

Isosurfaces of the second and third eigen values of the structure tensor of the image.

Results (1/3)

Segmentation/Reconstruction results

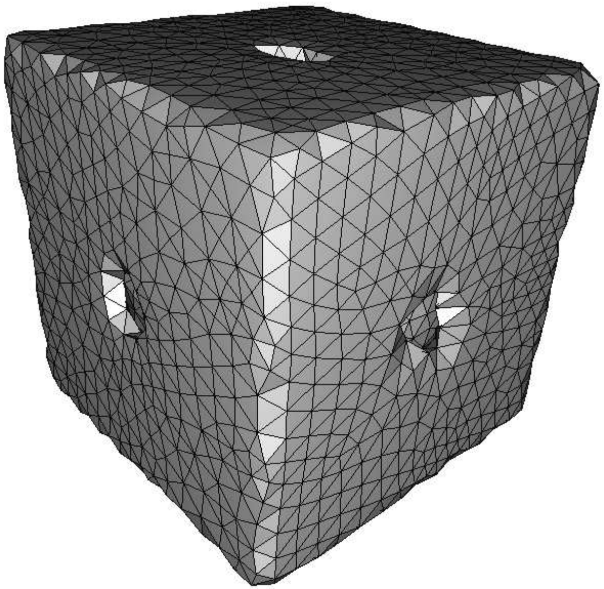

2163 vertices,
$\delta = 2, \zeta = 2.5$

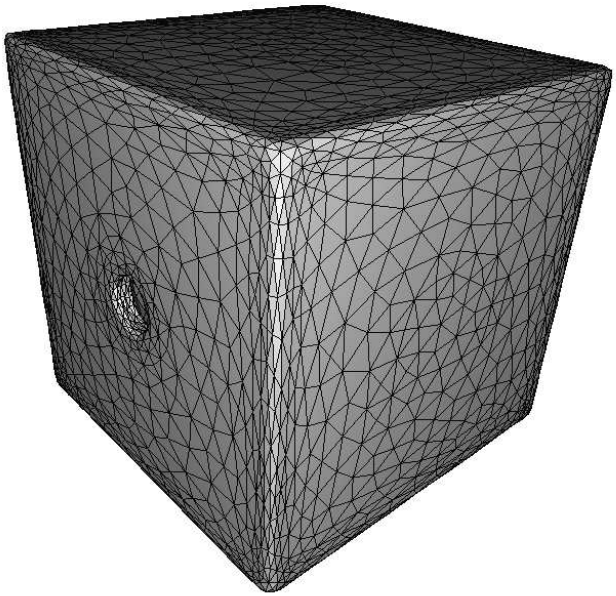

3497 vertices,
$\delta = 3, \zeta = 2.5,$
$1 \leq \sqrt{\mu_2} \leq \sqrt{\mu_1} \leq \sqrt{\mu_0} \leq 10$

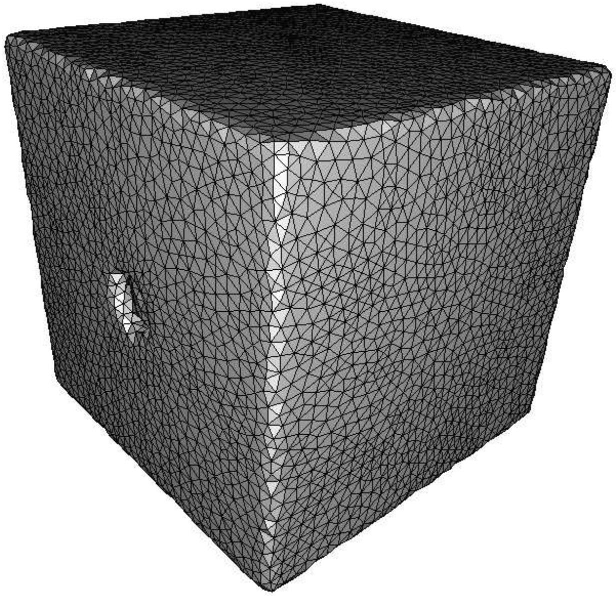

8904 vertices
$\delta = 1, \zeta = 2.5$

Results (1/3)

One corner of the cube

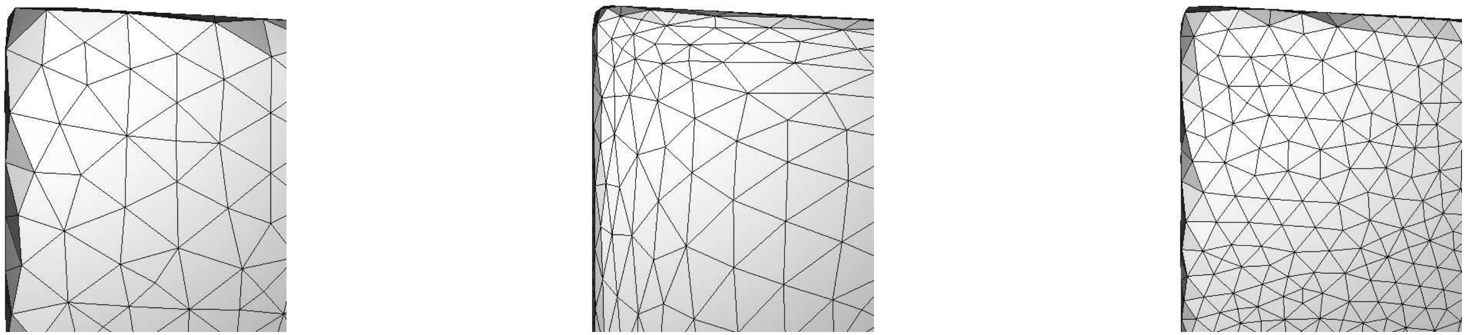

Hole in the cube

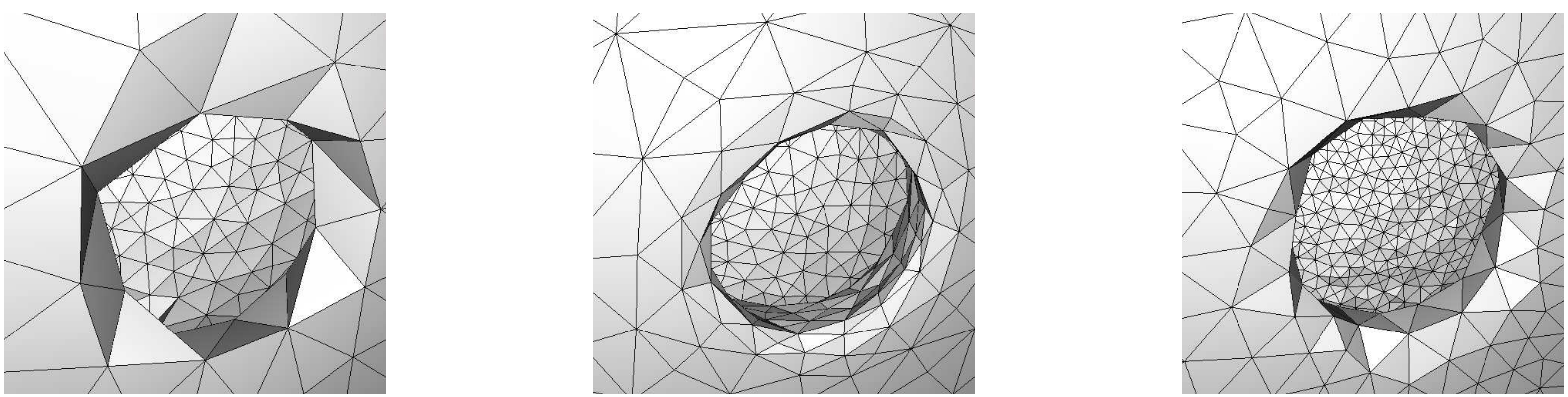

Results (1/3)

Repartition of edge lengths

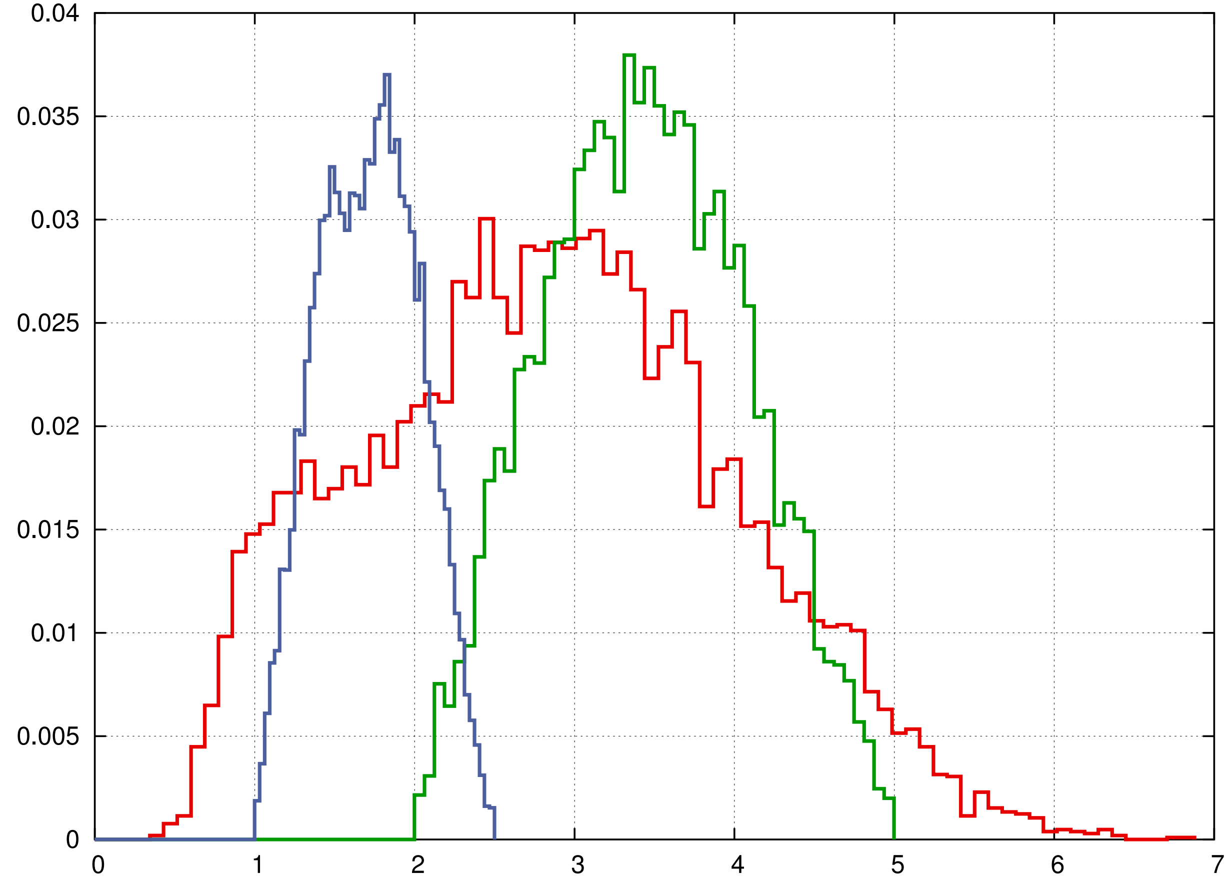

• fine model, • adaptive model, • coarse model

Results (2/3)

Computer generated image

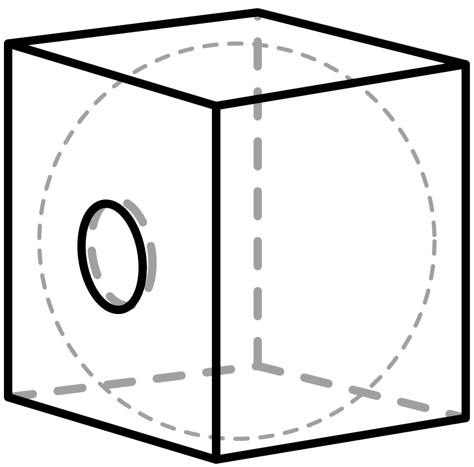

Object represented in the image

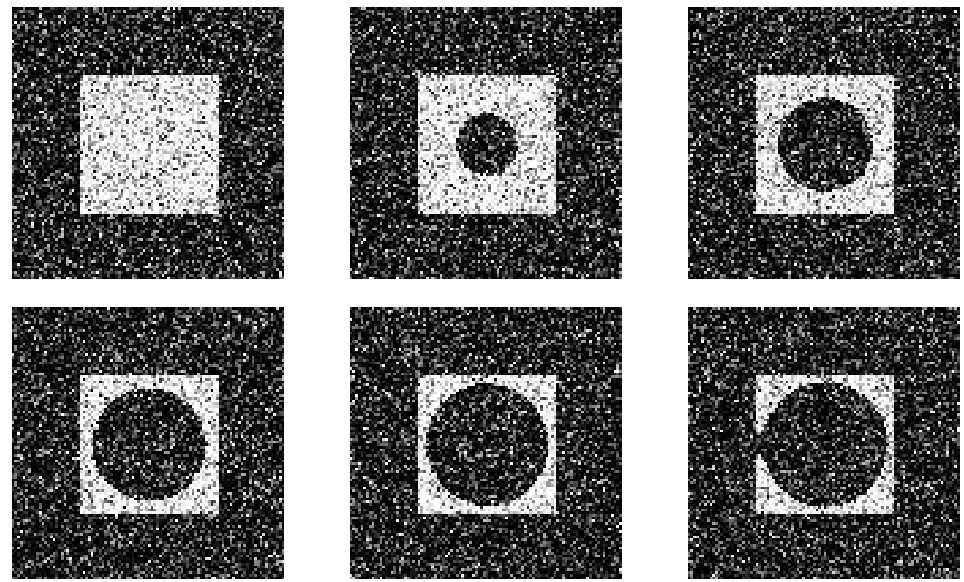

Slices extracted from the image

Results (2/3)

Eigen decomposition of the structure tensor

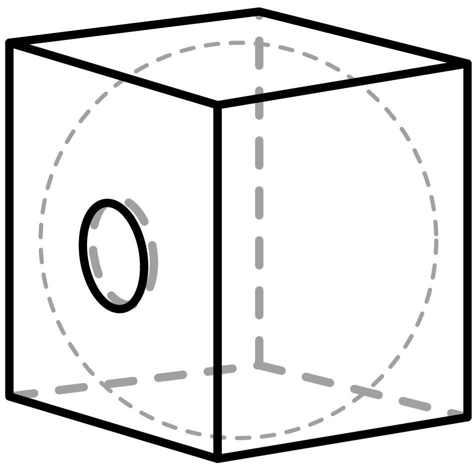

Object represented in the image

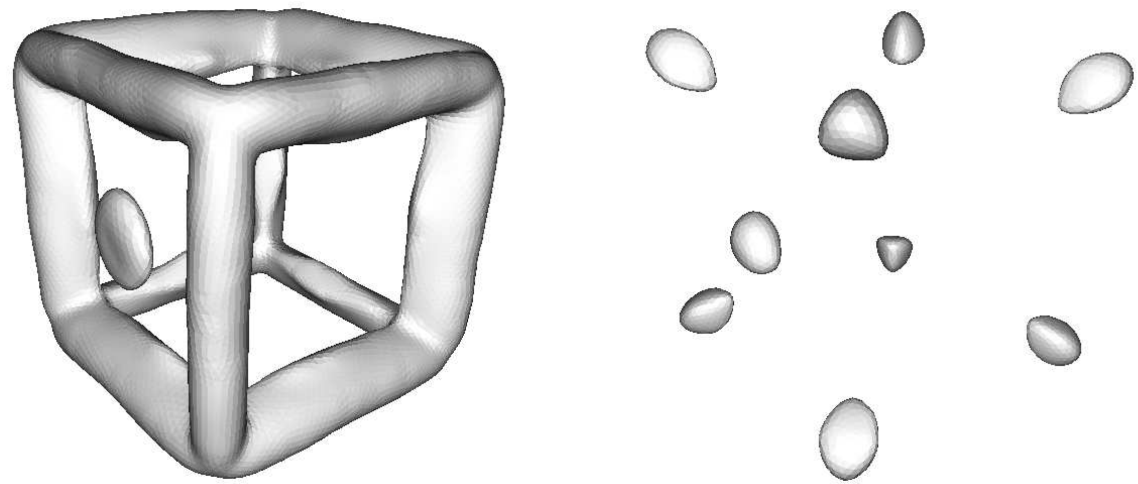

Isosurfaces of the second and third eigen values of the structure tensor of the image.

Results (2/3)

Segmentation/Reconstruction results

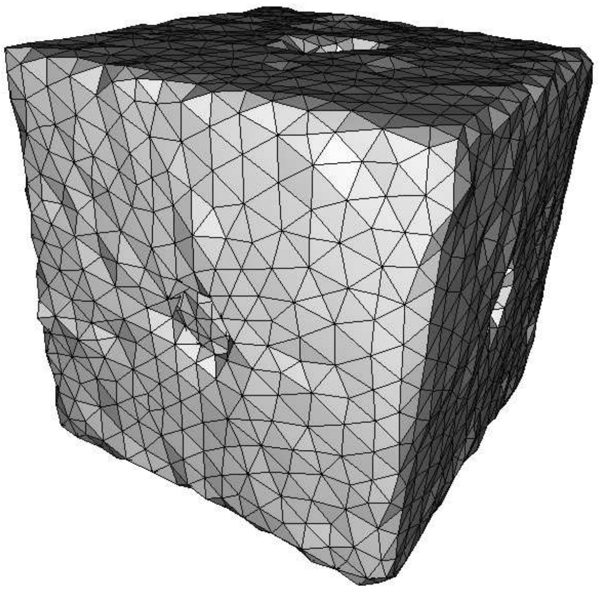

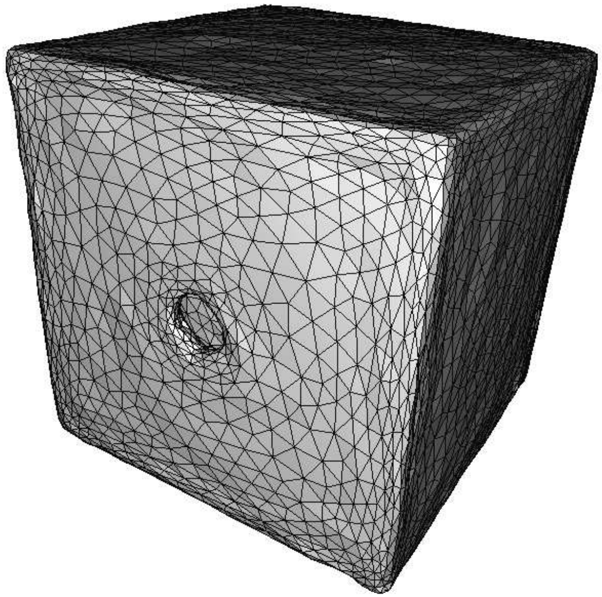

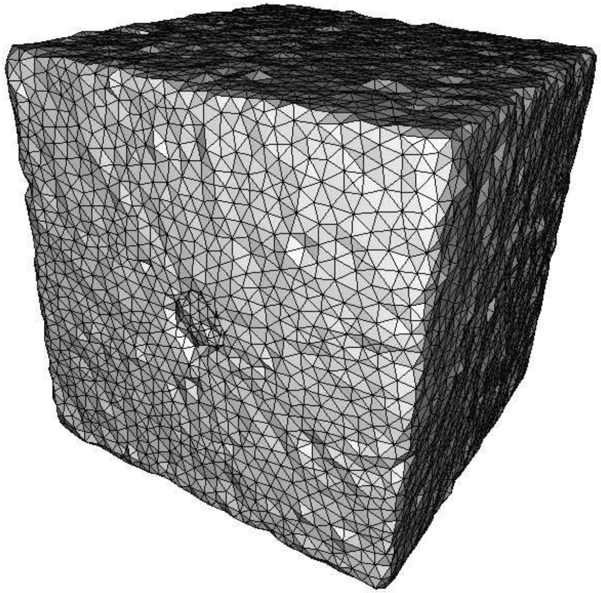

2107 vertices
$\delta = 2, \zeta = 2.5$

4832 vertices
$\delta = 3, \zeta = 2.5,$
$1 \leq \sqrt{\mu_2} \leq \sqrt{\mu_1} \leq \sqrt{\mu_0} \leq 10$

8542 vertices
$\delta = 1, \zeta = 2.5$

Results (2/3)

Repartition of edge lengths

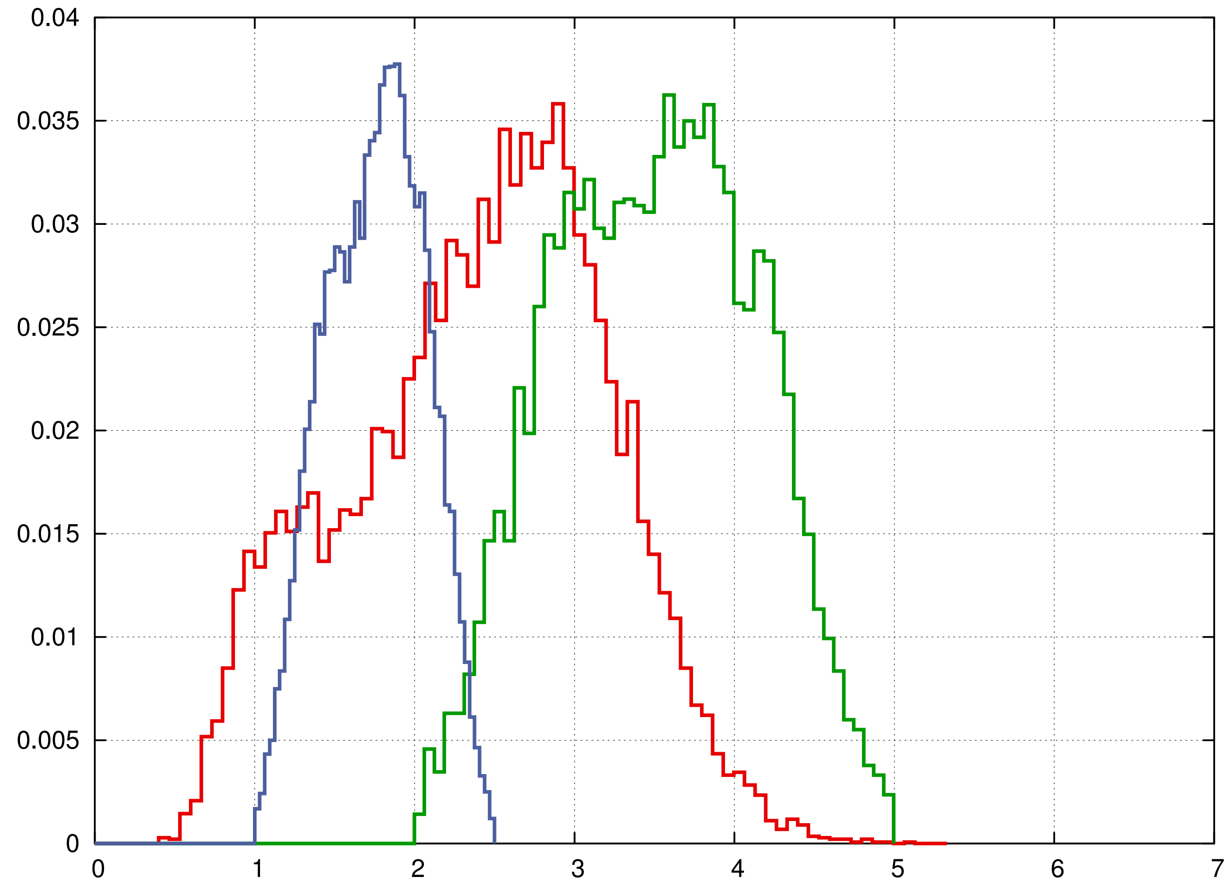

• fine model, • adaptive model, • coarse model

Results (3/3)

Biomedical image (Head CT-scan)

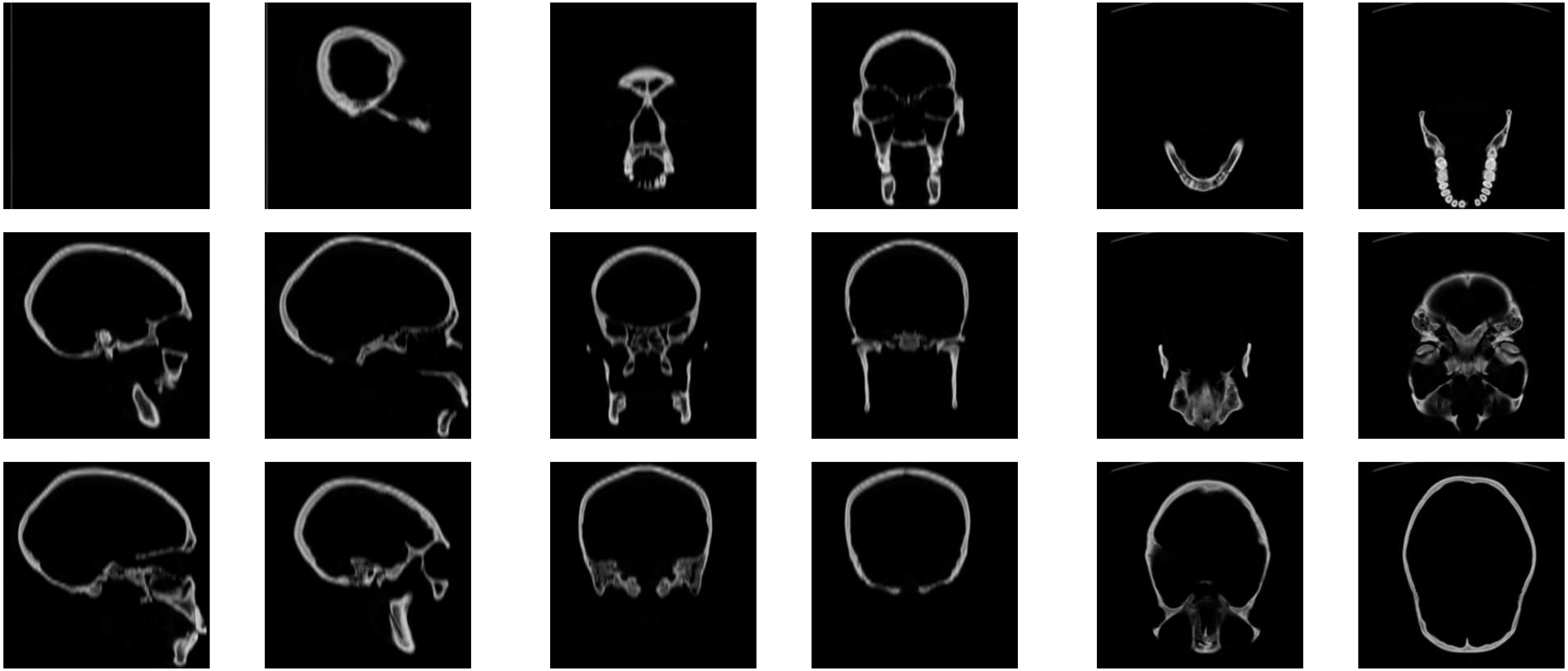

Results (3/3)

Eigen decomposition of the structure tensor

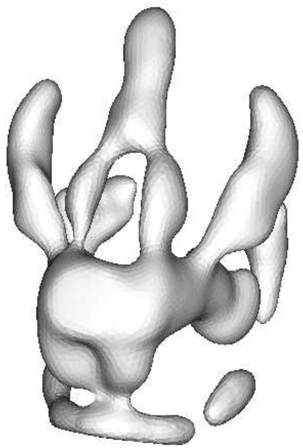

An isosurface of the 2nd eigenvalue.

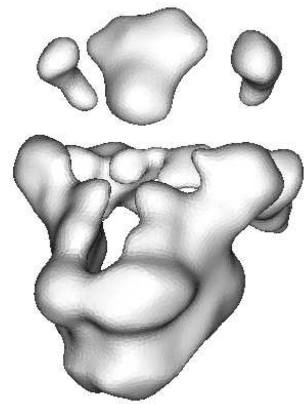

An isosurface of the 3rd eigenvalue.

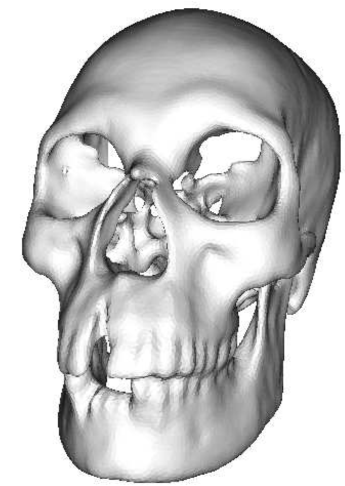

Object in the image.

Results (3/3)

Segmentation/Reconstruction results

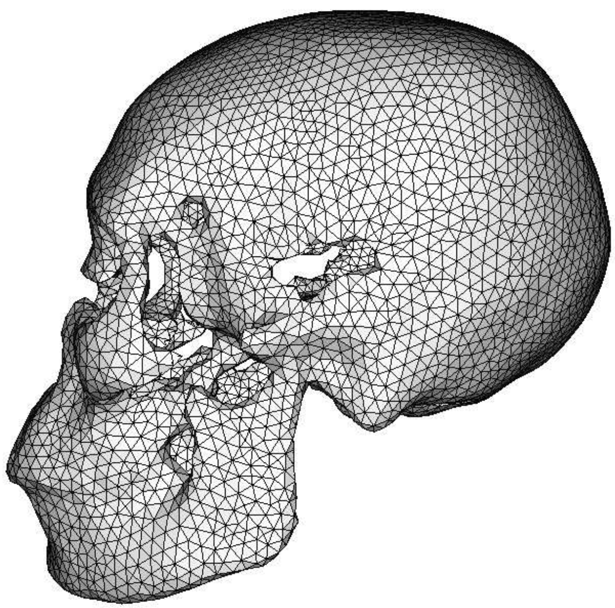

10.970 vertices
$\delta = 0.012, \zeta = 2.5$

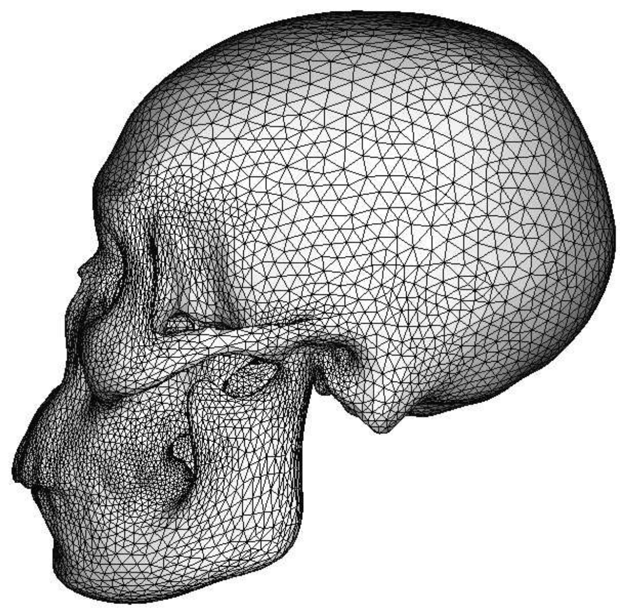

23.142 vertices
$\delta = 0.024$, $\zeta = 2.5$,
$1 \leq \sqrt{\mu_2} \leq \sqrt{\mu_1} \leq \sqrt{\mu_0} \leq 15$

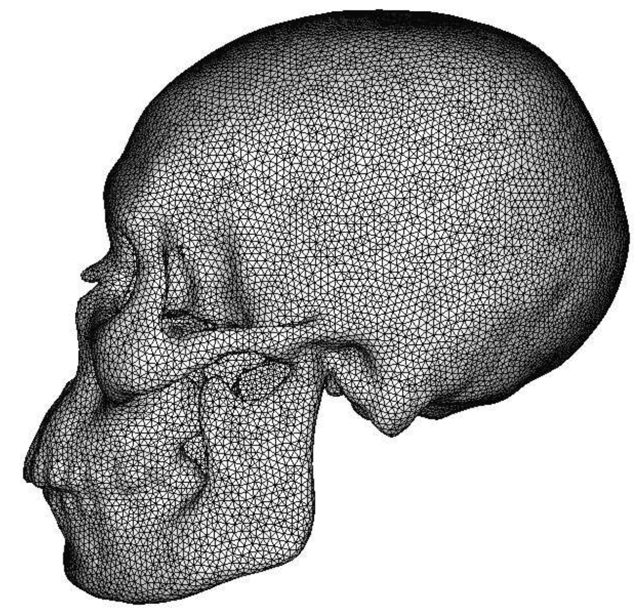

46.590 vertices,
$\delta = 0.005$, $\zeta = 2.5$

Results (3/3)

Left ear

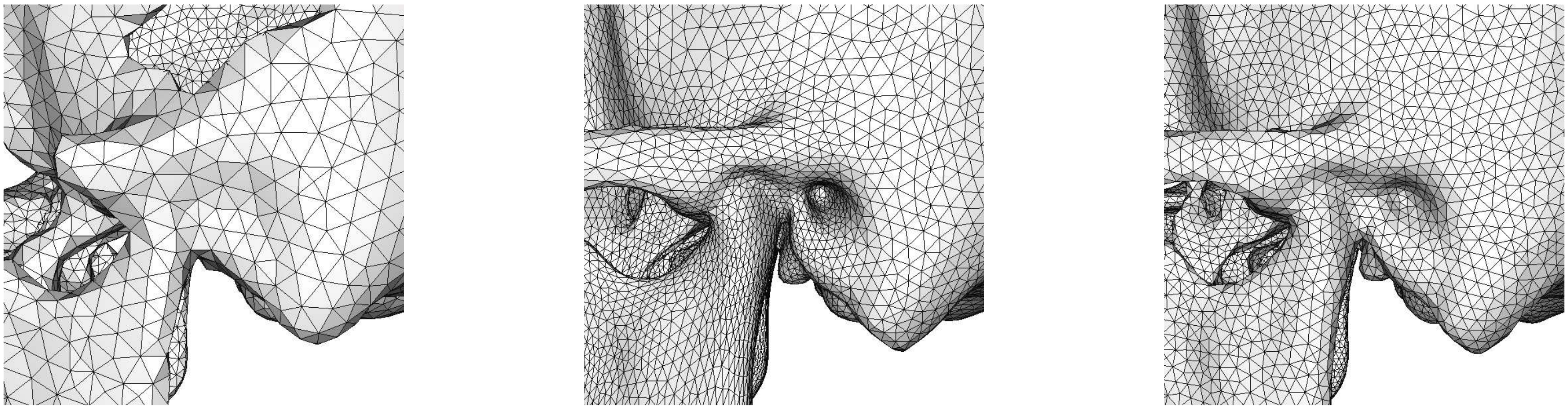

Orbit of the left eye viewed from behind left

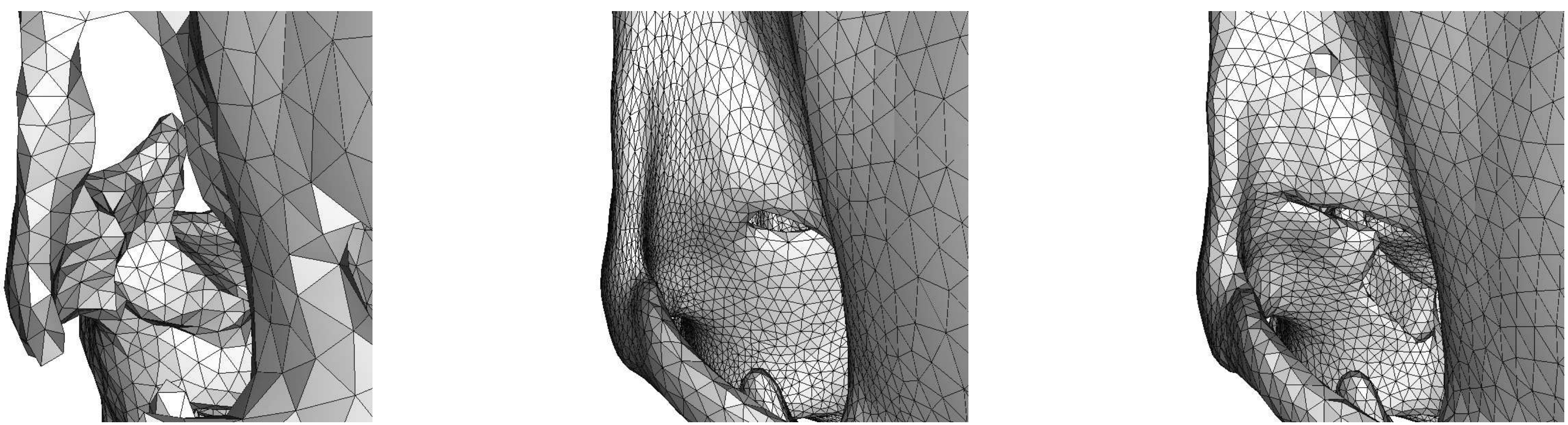

Results (3/3)

Repartition of the edge length

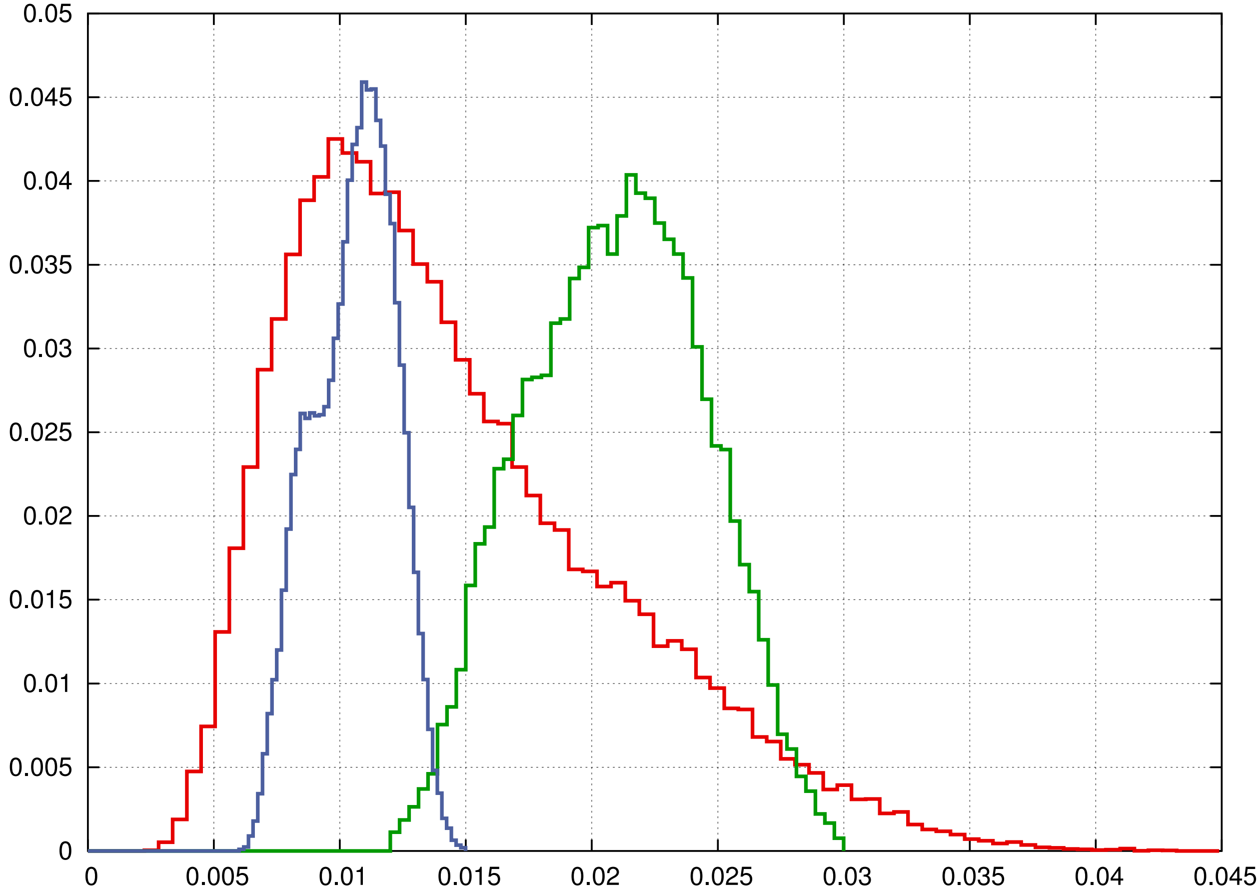

● fine model, ● adaptive model, ● coarse model

Conclusion and Perspectives

Conclusion

- Deformable model that achieves both
  - adaptive topology,
  - adaptive resolution

Perspectives

- Initialization with adaptive resolution,
- Different ways of building metrics. . .